RSC Advances

ROYAL SOCIETY OF CHEMISTRY

www.rsc.org/advances

Vibrational spectroscopy of isolated copper(II) complexes with deprotonated triglycine and tetraglycine peptides

Brett M. Marsh, Jia Zhou and Etienne Garand*

Department of Chemistry, University of Wisconsin, 1101 University Avenue, Madison, Wisconsin 53706, United States

*Author to whom correspondence should be addressed

email: egarand@chem.wisc.edu

Abstract

The gas-phase vibrational predissociation spectra of deprotonated copper-triglycine ($[Cu+G_3-3H]^-$) and deprotonated copper-tetraglycine ($[Cu+G_4-4H]^{2-}$), a known water oxidation catalyst, are presented. Unambiguous determination of the coordination structure in these complexes is made by comparison of the experimental spectra with calculations. We found both complexes to have an approximately square planar geometry in which all the amide groups are deprotonated and coordinating to the Cu center. Our experimentally determined structure for $[Cu+G_3-3H]^-$, in which the terminal carboxylate and amine groups provide the additional coordination interaction, agrees with previous studies. However, the $[Cu+G_4-4H]^{2-}$ complex is found to have the carboxylate group coordinated to the Cu center rather than NH_2, as determined in previous solution-phase studies. Our results also highlight the sensitivity of the amidate C=O stretch frequencies to the charge and coordination environment in these complexes. The observed experimental frequencies alone are capable of providing qualitative information on the interactions present in these species.

Keywords:

Water oxidation catalyst

Copper catalyst

Infrared spectroscopy

Density functional theory

Introduction

Copper is an earth-abundant and biorelevant transition metal with a ubiquitous presence in homogeneous and heterogeneous catalysis. Particularly, the ability of copper containing enzymes to reduce oxygen[1, 2] has led to recent discoveries of several nitrogen ligated copper catalysts that show promise for oxygen reduction and water oxidation.[3-6] One such catalyst, consisting of a Cu(II) center coordinated with a deprotonated tetraglycine molecule, has been found to have remarkable activity towards water oxidation.[6] This complex, noted for its proton transfer[7, 8] and oxidative properties[9], has been studied via X-ray crystallography[10], solution-phase electron paramagnetic resonance (EPR)[11] and solution-phase infrared (IR) spectroscopy[12]. However, in the condensed phase, spectral analysis and structural assignment is complicated by the simultaneous presence of several pH-dependent species as well as perturbations arising from interactions with counter-ions. On the other hand, gas phase vibrational spectroscopy is capable of isolating the species of interest to probe the structure and interactions in detail. Such studies have been carried out for a variety of amino acids,[13-15] peptides,[16-23] as well as metallated amino acids and peptides[24-27].

In this paper, we present the infrared vibrational predissociation[18, 28] study of isolated Cu(II) triglycine complex $[Cu+G_3-3H]^-$ and tetraglycine complex $[Cu+G_4-4H]^{2-}$. The species are isolated using electrospray ionization and cryogenically cooled prior to photo predissociation, yielding well-resolved vibrational spectra and allows for detailed comparison with density functional theory (DFT) calculations. Particular attentions are paid to the C=O and N-H stretch frequencies, which have been found to be highly indicative of molecular structures and

intramolecular interactions in previous solution and gas phase investigations.[24, 29] Furthermore, comparison of the amidate C=O stretch modes in $[Cu+G_3-3H]^-$ and $[Cu+G_4-4H]^{2-}$ showed notable sensitivity to the Cu bonding environment.

II. Experiment

Vibrational predissociation spectra of D_2-tagged $[Cu+G_3-3H]^-$ and $[Cu+G_4-4H]^{2-}$ complexes were obtained using a cryogenic ion photofragmentation mass spectrometer, described previously.[30] Briefly, ions of interest were generated via electrospray ionization (ESI) of a 1 mM $CuSO_4$ solution containing 1 mM triglycine (or tetraglycine) in a 65:35 acetonitrile:water mixture. The solution was adjusted to a pH of 9 with KOH, similar to previous work on these complexes.[11, 12, 31] The gas-phase ions were guided through three differentially pumped stages and collected in a 3D quadrupole ion trap (Jordan TOF) attached to a closed-cycle helium cryostat (Sumitomo) held at 10K by a resistive heater. A buffer gas of 10% D_2 in a balance of helium was pulsed into the trap for collisional cooling and condensation of D_2 tags onto the ions. These weakly bound (binding energy ~100-300 cm^{-1}) D_2 molecules serve as messenger for the vibrational spectroscopy. Extraction into the time-of-flight mass spectrometer allowed the tagged ions with m/z = 257, corresponding to $[^{63}Cu+G_3-3H]^-\cdot(D_2)_2$ (or m/z = 158.5 for $[^{63}Cu+G_4-4H]^{2-}\cdot(D_2)_3$), to be isolated using a mass gate, and intersected with the output of an infrared OPO/OPA laser system (LaserVision). When the IR photon energy is resonant with a vibrational transition, the absorption of a single photon is sufficient to induce the evaporation of the weakly bound D_2 tags. The photofragment ions corresponding to the loss of all D_2 tags were separated from the parent ions in a two-stage reflectron. The resulting

photofragment intensity as a function of the photon energy yielded linear IR spectra. The final intensities are normalized to laser output power.

Electronic structure calculations were carried out using Gaussian 09.[32] Optimized geometries and harmonic frequencies of the gas phase species were calculated at the cam-B3LYP/6-311++G(d,p) level. The reported relative energies include zero-point corrections. The harmonic vibrational frequencies were scaled by a factor of 0.959 for the 1200-1800 cm^{-1} range, and 0.948 for the 2800-3600 cm^{-1} range. These scaling factors were obtained by comparing calculated values (cam-B3LYP/6-311++G(d,p)) of the N-H and C=O stretch frequencies of N-methyl acetamide with their experimental values.[33] It should be noted that calculations yielded very similar vibrational spectrum for the bare and tagged species, with the major difference being the additional presence of the weak D_2 stretch band. For simplicity, the calculated results of the bare complexes are used for the analysis of experimental spectra.

III. Results

The gas-phase vibrational predissociation spectrum of $[Cu+G_3-3H]^-$ in the 1200-1800 cm^{-1} and 2800-3600 cm^{-1} range is shown in Figure 1. The three strongest features appear in the C=O stretch region at 1632 cm^{-1}, 1654 cm^{-1} and 1672 cm^{-1}. Four weak features are observed at lower frequencies, at 1252 cm^{-1}, 1293 cm^{-1}, 1380 cm^{-1} and 1393 cm^{-1}. All the features in the higher frequency region are very weak. Several peaks are observed in the 2800-3000 cm^{-1} region where the CH stretch modes and the D_2 stretch mode are expected to appear. The nominally forbidden D_2 stretch becomes weakly allowed when the centrosymmetry is broken by binding to the ion. A single weak peak is found at 3408 cm^{-1} in the N-H stretch region.

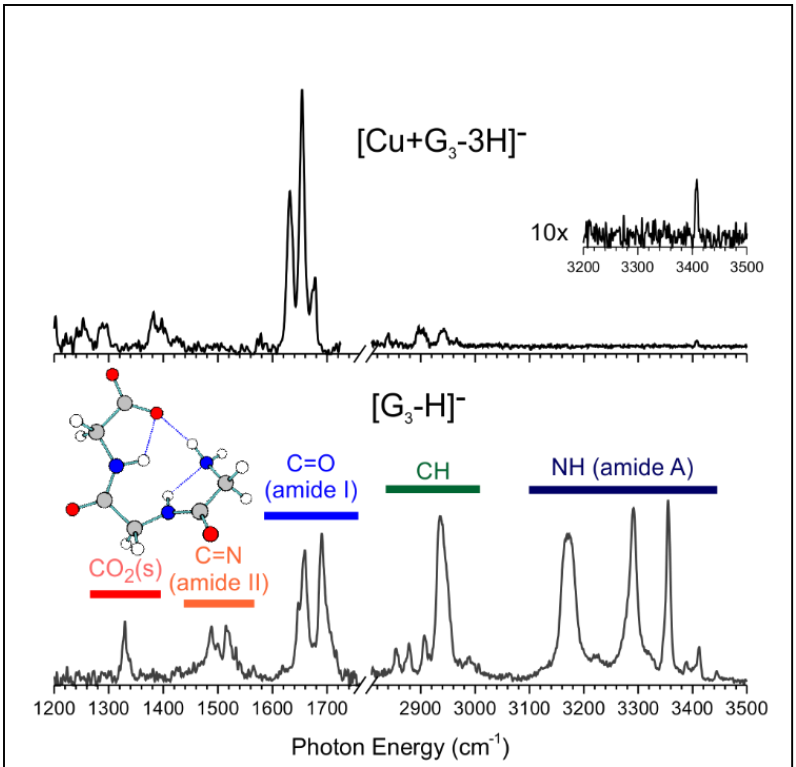

Figure 1. Experimental IR spectra of $[Cu+G_3-3H]^-$ (top) and $[G_3-H]^-$ (bottom). The spectrum of $[G_3-H]^-$ is analyzed in detail in ref.19.

The vibrational spectrum of the $[Cu+G_3-3H]^-$ complex can be compared to the spectrum of the singly deprotonated triglycine species $[G_3-H]^-$, presented in the bottom panel of Figure 1. The spectrum analysis and structure of this species has been described in detail previously.[19] Briefly, it forms a cyclic structure in which the terminal carboxylate and NH_2 groups are linked by hydrogen bonding. Cursory inspection of the spectra in Figure 1 reveals several differences between the two species. First, the three intense peaks between 3100 cm^{-1} and 3400 cm^{-1} in the $[G_3-H]^-$ spectrum, assigned to the two hydrogen-bonded amide N-H and the hydrogen-bonded N-H in NH_2, are completely absent in $[Cu+G_3-3H]^-$. The experimental spectrum of $[Cu+G_3-3H]^-$ only displays a single weak peak in the free N-H region. In the lower frequency region, between 1450 cm^{-1} and 1550 cm^{-1}, the peaks assigned to the amide II modes in $[G_3-H]^-$ are also absent in $[Cu+G_3-3H]^-$. The amide II mode in peptides contains significant contributions from N-H bending motion.[29] The disappearance of the amide A and amide II features clearly indicate the deprotonation of both amides in the $[Cu+G_3-3H]^-$ complex. Another notable difference between the two species is the ~25 cm^{-1} redshift of the peaks in the

C=O stretch region of $[Cu+G_3-3H]^-$ compared to $[G_3-H]^-$. This effect has been observed in previous studies of metallated peptides.[12, 34]

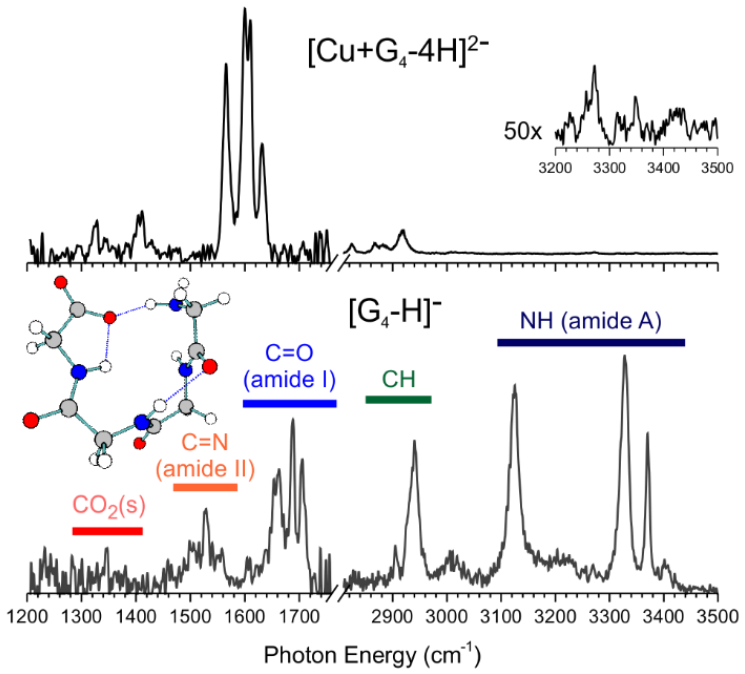

Figure 2. Experimental IR spectra of $[Cu+G_4-4H]^-$ (top) and $[G_4-H]^-$ (bottom). The spectrum of $[G_4-H]^-$ is analyzed in detail in ref. 19.

The gas-phase vibrational predissociation spectrum of $[Cu+G_4-4H]^{2-}$, in the 1200-1800 cm^{-1} and 2800-3600 cm^{-1} range, is shown in Figure 2. It is qualitatively similar to the spectrum of the $[Cu+G_3-3H]^-$ complex. The predominant feature is a set of four intense peaks at 1566 cm^{-1}, 1601 cm^{-1}, 1609 cm^{-1} and 1632 cm^{-1}. Two additional weaker features are observed at 1326 cm^{-1} and 1407 cm^{-1}. Again, only weak features are found in the higher frequency region. A group of peaks is observed between 2800 cm^{-1} and 3100 cm^{-1} where the CH stretch and nominally forbidden D_2 stretch vibrations are expected. Very little activity is found in the N-H region, with only two very weak peaks at 3271 cm^{-1} and 3351 cm^{-1}.

The vibrational spectrum of the $[Cu+G_4-4H]^{2-}$ complex can be compared with the spectrum of the singly deprotonated tetraglycine species $[G_4-H]^-$, presented in the bottom panel of Figure 2. The structure of this species, which has been described in detail previously,[19]

is also cyclic in which the terminal carboxylate and NH_2 groups are linked by hydrogen bonding. Comparison of the $[Cu+G_4-4H]^{2-}$ and $[G_4-H]^-$ spectra shows the same trends observed for the triglycine species. The most apparent difference is the disappearance of the intense hydrogen-bonded N-H stretch peaks in the 3100-3400 cm^{-1} range which again suggest that all three amide groups of the tetraglycine ligand are deprotonated in $[Cu+G_4-4H]^{2-}$. Lastly, the redshift of the C=O stretch peaks in $[Cu+G_4-4H]^{2-}$ compared to $[G_4-H]^-$ is ~90 cm^{-1}, significantly more than that of the triglycine species.

IV. Analysis

From the experimental spectra presented in the previous section, it appears that all the amide groups are deprotonated in $[Cu+G_3-3H]^-$ and $[Cu+G_4-4H]^{2-}$. Therefore, only starting geometries in which the amide and carboxylic acid groups are deprotonated were considered in the electronic structure calculations. For the $[Cu+G_3-3H]^-$ complex, all the starting geometries converged to the same structure, shown in Figure 3, in which the triply deprotonated triglycine ligand wraps around Cu(II) metal center in an approximately square planar geometry. The peptide is bound to the Cu via one of the carboxylate oxygens, the two nitrogens of the amidate groups and the nitrogen of the terminal NH_2 group. This geometry agrees well with the structure obtained from solution phase measurements.[11, 12] To facilitate the discussion, we label the two amidate groups α and β, starting from the terminal carboxylate.

The calculated vibrational spectrum (Figure 3 bottom panel) has an excellent agreement with the experimental spectrum, allowing for unambiguous assignment of the observed features. In the C=O stretch region, the peaks at 1675 and 1654 cm^{-1} are assigned to a mixture

of the CO_2 antisymmetric stretch and the β-C=O stretch. The feature at 1632 cm^{-1} is assigned to the α-C=O stretch. The two peaks at 1380 cm^{-1} and 1393 cm^{-1} are assigned to CH_2 bending motions. The lower frequency peak at 1293 cm^{-1} is assigned to a mixture of the CO_2 symmetric stretch and CH_2 wag modes. The features in the region of 2800-3100 cm^{-1} can be assigned to various CH_2 stretching modes. The peak at 2942 cm^{-1}, which is absent in the calculation, is assigned to the D_2 stretch of the tags. This frequency is close to the free D_2 stretch at 2994 cm^{-1}, indicating very weakly interacting tags. Finally, the weak feature at 3408 cm^{-1} can be assigned to the antisymmetric stretch of the NH_2 group. The corresponding symmetric NH_2 stretch, calculated to appear at 3353 cm^{-1}, is significantly weaker than the antisymmetric stretch and is not observed in the experimental spectrum.

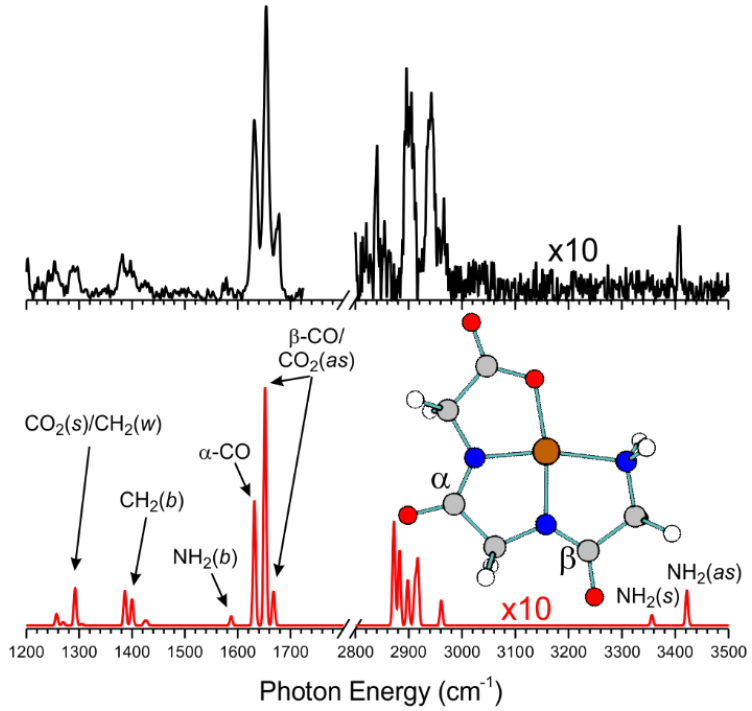

Figure 3. Experimental (top) and calculated (bottom) spectra of the $[Cu+G_3-3H]^-$ complex. For both spectra, the intensity in the 2800-3500 cm^{-1} region is multiplied by 10 to clearly show the weak features. For the labels: *as*=antisymmetric stretch, *s*=symmetric stretch, *b*=bend, *w*=wag. The position of the α and β amide group is indicated on the structure.

Calculations revealed four low-lying structures for the $[Cu+G_4-4H]^{2-}$ complex. The structures are shown in Figure 4 (I-IV), along with their respective calculated spectra. Once again, we label the three amidate groups α, β and γ, starting from the terminal carboxylate. All

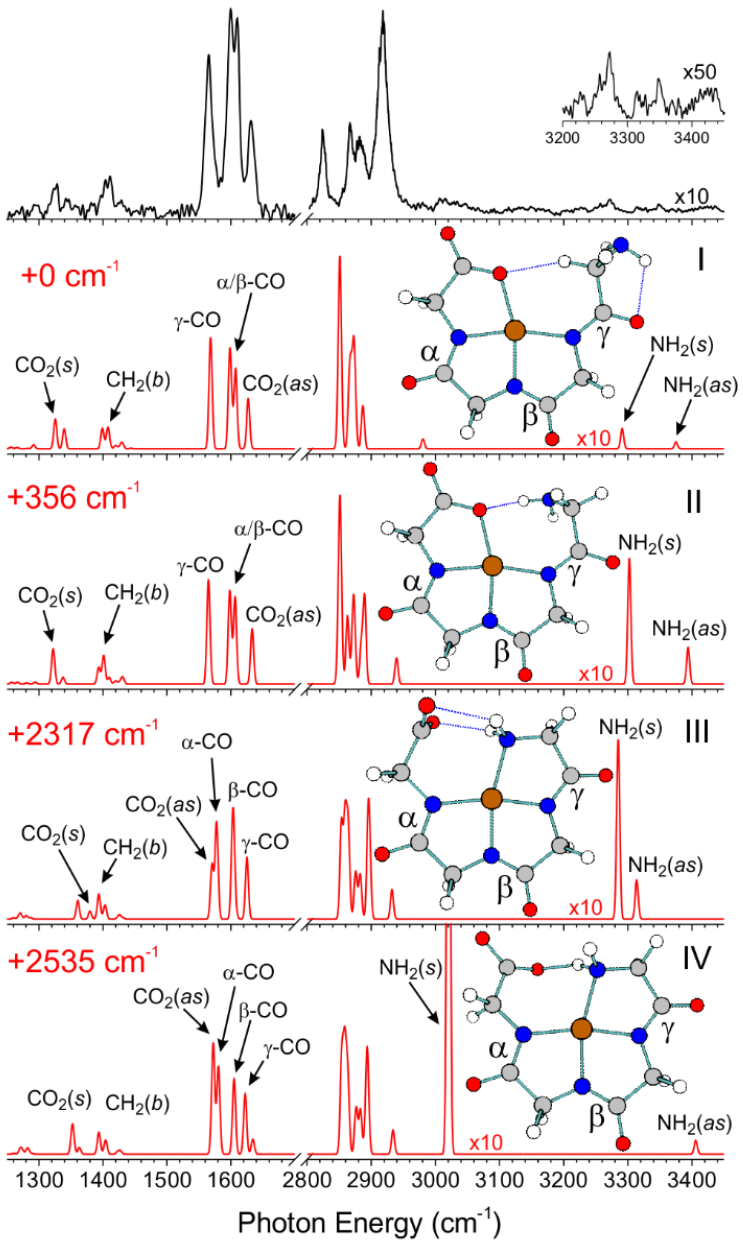

Figure 4. Experimental (top) and calculated (I-IV) spectra of the $[Cu+G_4-4H]^-$ complex. For all spectra, the intensity in the 2800-3500 cm^{-1} region is multiplied by 10 to clearly show the weak features. For the labels: *as*=antisymmetric stretch, *s*=symmetric stretch, *b*=bend, *w*=wag. The position of the α, β, and γ amide group is indicated on the structures.

four conformers have an approximately square planar geometry with the three nitrogen on the amidate groups bound to the Cu center. In the two lowest energy structures (I and II), the fourth coordination comes from the carboxylate oxygen. In conformer I, the NH_2 is weakly interacting with the neighboring γ-C=O. In conformer II, calculated to be 356 cm^{-1} higher in energy, the NH_2 is hydrogen bonded to the carboxylate group. In conformers III and IV, calculated to be 2319 cm^{-1} and 2535 cm^{-1} higher in energy, respectively, the fourth coordination is with the NH_2 group. For both structures, the

carboxylate is hydrogen bonded to the NH_2 group. This coordination motif is similar to those assigned in previous work on $[Cu+G_4-4H]^{2-}$.[11, 12]

In the C=O stretch region, 1550-1650 cm^{-1}, the calculated spectra for conformers I and II are very similar, and both show excellent agreement with the experimental spectrum. On the other hand, the peak pattern in the C=O region of conformers III and IV do not agree as well with the experiment. There are further differences between the calculated spectra in the 3000-3500 cm^{-1} N-H stretch region. For conformers II-IV, N-H stretch features with intensities comparable to or greater than the C-H stretch modes (2800-2900 cm^{-1}) are present at various frequencies. This is clearly not observed in the experimental spectrum. Only conformer I is calculated to have the correct relative intensities for the symmetric and antisymmetric NH_2 stretch modes. The calculated frequencies are also in good agreement with the two observed very weak features at 3271 cm^{-1} and 3351 cm^{-1}. These clear differences allow us to rule out the presence of conformers II-IV and assign all observed features to conformer I.

In the C=O stretch region, the feature at 1632 cm^{-1} is assigned to the CO_2 antisymmetric stretch. The doublet at 1609 and 1601 cm^{-1} correspond to a mixture of the α and β C=O stretch and the peak at 1566 cm^{-1} is assigned to the γ-C=O stretch. The peak at 1407 cm^{-1} corresponds to the CH_2 bending vibrations whereas the feature at 1325 cm^{-1} corresponds to the CO_2 symmetric stretch. The features between 2800 and 2900 cm^{-1} are assigned to various CH_2 symmetric and antisymmetric stretch modes. The large feature at 2917 cm^{-1}, which is absent in the calculated spectrum, is assigned to the D_2 stretch mode of the tags. This frequency is again close to the free D_2 stretch, but slightly redshifted compared to those in $[Cu+G_3-3H]^-$. The D_2

tag frequency difference indicate a stronger binding energy to the doubly charged $[Cu+G_4-4H]^{2-}$ than the singly charged $[Cu+G_3-3H]^-$. This is confirmed by calculations which show that the D_2 tags have a binding energy of about 100 cm^{-1} (1.2 kJ/mol) in $[Cu+G_3-3H]^-\cdot D_2$ compared to 300 cm^{-1} (3.6 kJ/mol) in $[Cu+G_4-4H]^{2-}\cdot D_2$.

V. Discussion

The four-fold coordination present in the $[Cu+G_3-3H]^-$ and $[Cu+G_4-4H]^{2-}$ complexes is similar to other Cu(II) complexes.[30, 35] It also agrees with previous studies of these species in the solution phase.[11, 12] However, for $[Cu+G_4-4H]^{2-}$, the solution phase studies concluded that the four equatorial coordination groups are the three amidates and the NH_2 group, with structures similar to conformer III and IV. Specifically, in the EPR experiments performed by Nagy et al.,[11] the carboxylate group is determined to not directly interact with the copper center. This geometry was based on various ESR parameters extracted from spectral deconvolution. In the solution-phase IR spectroscopy work of Kim and Martell,[12] it was determined that the carboxylate group resided on the axial position. This was based on the observation of two amide I bands at 1610 cm^{-1} and 1570 cm^{-1}, which were assigned to the amidate C=O and a weakly coordinated carboxylate group, respectively. However, no such stable geometry could be found in our calculation search. In order for the carboxylate to reach the axial coordination position, the α-amidate group has to be rotated out the equatorial plane, severely straining its bond with the copper. In addition, the calculated spectra in Figure 4 show that geometries involving either NH_2 or CO_2 coordination at the fourth equatorial site would produce IR spectra with very similar appearance in the C=O region, especially at low resolution.

The non-coordinating CO_2 in conformers III and IV does indeed appear at ~1570 cm^{-1}, but at the same time, all the conformers are predicted to have an amidate C=O band at about the same frequency.

This different coordination motif observed in our experiments can be explained by several experimental parameters. For instance, we use an acetonitrile/water mixture rather than a pure aqueous solution. However, the most obvious reason is that our measurements were carried out in the gas phase where all the solvents are removed. In order to investigate the effect of solvation on the geometry, we have performed additional calculations on the $[Cu+G_4-4H]^{2-}$ complex to include implicit water and acetonitrile solvent interactions through the PCM model[36]. We found the same four low energy structures as shown in Figure 4, and interestingly, the PCM results indicate that conformers I and IV are the two lowest energy conformers in solution and they are nearly isoenergetic. Conformer I is still the lowest energy conformer by 45 cm^{-1} (0.49 kJ/mol) in acetonitrile, but we found conformer IV to be the ground state by 21 cm^{-1} (0.25 kJ/mol) in water. Such large relative solvent stabilization of conformer IV, in which the NH_2 group is coordinated to the metal, thus provide the likely cause of the different structure found here. The large solvation energy of the charged carboxylate compared to the neutral NH_2 makes it less favorable to be coordinated in solution. However in the absence of any solvent, the carboxylate coordinated conformer I becomes more energetically favorable. The small calculated energy differences between conformer I and IV would suggest that both species might be present in solution. More accurate determination of the relative energy of these conformers would require the inclusion of explicit solvent molecules which is beyond the scope of the present work. However, we note that the fact that

we only observe conformer I in our experimental spectrum suggest that the barriers between these structures is relatively small and easily overcome during the electrospray ionization or collisional cooling process in the ion trap.

Also of interest is the sensitivity of the C=O stretch bands to the coordination environment of the Cu(II) complex. This is illustrated in Figure 5, which focuses on the 1300-1800 cm^{-1} region of both $[Cu+G_3-3H]^-$ and $[Cu+G_4-4H]^{2-}$ species. For comparison, Figure 5 also includes the calculated C=O stretch frequencies of a free amide and a free amidate anion using N-methyl acetamide as a model. The free amidate C=O stretch has a calculated frequency of 1569 cm^{-1}, 138 cm^{-1} lower than the free amide C=O stretch (1707 cm^{-1}). The origin of this shift can be understood by examining the differences in bond lengths between the amide and amidate species. Upon deprotonation, the C=O bond length is increased from 1.217 Å to 1.264 Å, while the C-N bond is shortened from 1.358 Å to 1.313Å. This shows that the negative

charge is delocalized through a [$^{-}$O-C=N] ↔ [O=C-N^{-}] resonance structure. The C=O frequencies can therefore be used as a probe of the charge transfer upon coordination to the Cu center.

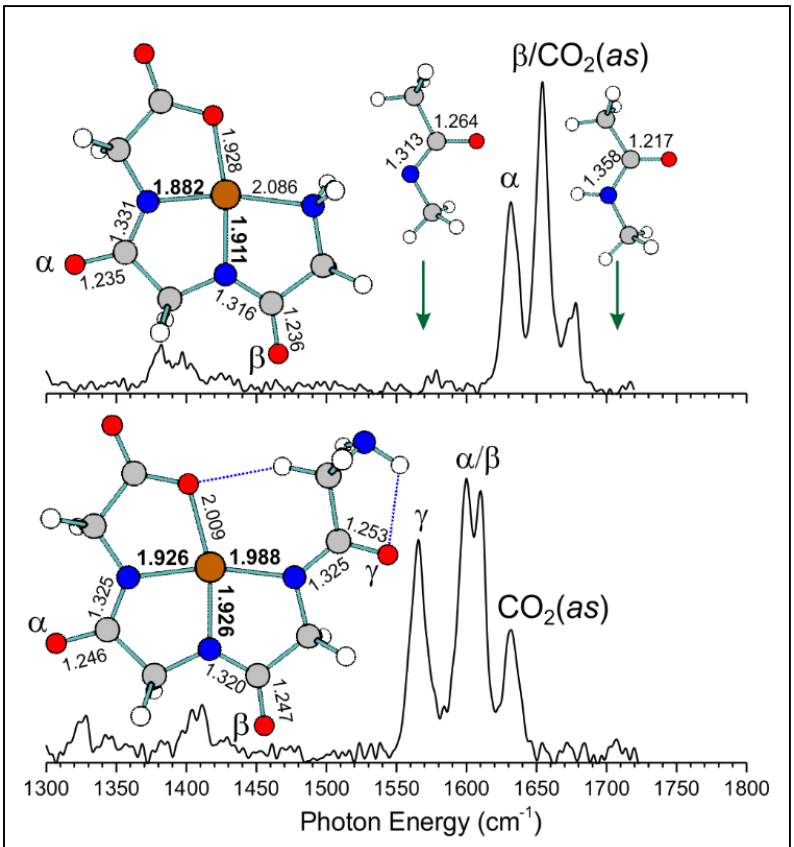

Figure 5. Experimental IR specta of [Cu+G$_3$-3H]$^{-}$ (top) and [Cu+G$_4$-4H]$^{2-}$ (bottom) in the amide I region. In each panel are the corresponding calculated (cam-B3LYP/6-311++G(d,p)) structure and bond lengths. Also shown are the free amide and amidate frequencies (green arrows) with calculated structures.

The observed C=O stretch modes in [Cu+G$_4$-4H]$^{2-}$ are at lower frequencies than their corresponding modes in [Cu+G$_3$-3H]$^{-}$. This implies that each amidate group in [Cu+G$_4$-4H]$^{2-}$ has less charge transfer to the Cu center and a structure that is closer to the free amidate anion. The calculated geometries, shown in Figure 5, agree with that assessment. Notably, the Cu-N bond lengths in [Cu+G$_4$-4H]$^{2-}$ are all longer than those in [Cu+G$_3$-3H]$^{-}$. Upon closer inspection, we can see that the γ-amidate in [Cu+G$_4$-4H]$^{2-}$ has the longest Cu-N bond length of 1.988 Å, and its C=O stretch is the lowest frequency at 1566 cm^{-1}. This C=O stretch is not significantly perturbed by its weak interaction with the NH$_2$ group, as shown by conformer II in Figure 4 which has a similar frequency for its free γ-C=O stretch. The two other amidate groups in [Cu+G$_4$-4H]$^{2-}$ have a Cu-N bond length of 1.926 Å, giving rise to similar C=O and C-N bond lengths and C=O stretches at similar frequencies around

1600 cm^{-1}. The shorter Cu-N bond lengths in $[Cu+G_3-3H]^-$, 1.882 Å and 1.911 Å, correspond to higher frequency C=O stretches at 1632 cm^{-1} and 1654 cm^{-1}. The stronger Cu-N interactions in $[Cu+G_3-3H]^-$ is likely due to the fact that there are only two amidate groups interacting with Cu. The total charge transfer to the copper center is spread over a smaller number of amidate groups, leading to a larger charge transfer per Cu-N bond. The amide I region is often considered to be diagnostic of the peptide structure.[29, 37] Here, we have shown the ability of well-resolved IR spectroscopy to yield information on the charge and coordination of metal-center complexes. This capability will be useful in future studies of related complexes involved in the water oxidation, as well as larger structures where detailed calculations are less feasible.

VI. Conclusions

The vibrational predissociation spectra of two isolated Cu(II) oligoglycine complexes, $[Cu+G_3-3H]^-$ and $[Cu+G_4-4H]^{2-}$, are presented. Analysis of the experimental spectra is aided by DFT calculations. For each species, a single structural conformer is responsible for all the observed features, all of which can be readily assigned. For $[Cu+G_3-3H]^-$, the two amidate, NH_2 and carboxylate groups are coordinated with the Cu center, in agreement with previous studies. On the other hand, the $[Cu+G_4-4H]^{2-}$ complex is found to have the carboxylate group as the fourth coordination in contrast to previous solution-phase assignments in which the NH_2 is involved in the coordination. However, electronic structure calculations with implicit solvent suggest that both species may be present in solution. Furthermore, we find the frequencies of the amidate C=O modes to be very sensitive to the charge and coordination environment of the

metal complexes. The observed experimental frequencies alone are capable of providing qualitative information on the interactions present in these complex species.

Acknowledgments

The authors acknowledge the Donors of the American Chemical Society Petroleum Research Fund for partial support of this research. The experimental setup used in this study was built using start-up funds from the UW Madison chemistry department. The computational resources used in this work are supported by National Science Foundation Grant CHE-0840494.

References:

1. E. A. Lewis and W. B. Tolman, *Chem. Rev.*, 2004, **104**, 1047-1076.
2. L. M. Mirica, X. Ottenwaelder and T. D. P. Stack, *Chem. Rev.*, 2004, **104**, 1013-1045.
3. S. M. Barnett, K. I. Goldberg and J. M. Mayer, *Nat Chem*, 2012, **4**, 498-502.
4. T. Zhang, C. Wang, S. Liu, J.-L. Wang and W. Lin, *J. Am. Chem. Soc.*, 2013, **136**, 273-281.
5. M. Zhao, H.-B. Wang, L.-N. Ji and Z.-W. Mao, *Chem. Soc. Rev.*, 2013, **42**, 8360-8375.
6. M. T. Zhang, Z. F. Chen, P. Kang and T. J. Meyer, *J. Am. Chem. Soc.*, 2013, **135**, 2048-2051.
7. M. P. Youngblood, K. L. Chellappa, C. E. Bannister and D. W. Margerum, *Inorg. Chem.*, 1981, **20**, 1742-1747.
8. M. P. Youngblood and D. W. Margerum, *Inorg. Chem.*, 1980, **19**, 3072-3077.
9. J. L. Kurtz, G. L. Burce and D. W. Margerum, *Inorg. Chem.*, 1978, **17**, 2454-2460.
10. H. C. Freeman and M. R. Taylor, *Acta Crystallographica*, 1965, **18**, 939-952.
11. N. V. Nagy, T. Szabo-Planka, A. Rockenbauer, G. Peintler, I. Nagypal and L. Korecz, *J. Am. Chem. Soc.*, 2003, **125**, 5227-5235.
12. M. K. Kim and A. E. Martell, *J. Am. Chem. Soc.*, 1966, **88**, 914-918.
13. D. Scuderi, C. F. Correia, O. P. Balaj, G. Ohanessian, J. Lemaire and P. Maitre, *Chemphyschem*, 2009, **10**, 1630-1641.
14. B. C. Dian, J. R. Clarkson and T. S. Zwier, *Science*, 2004, **303**, 1169-1173.
15. J. A. Stearns, S. Mercier, C. Seaiby, M. Guidi, O. V. Boyarkin and T. R. Rizzo, *J. Am. Chem. Soc.*, 2007, **129**, 11814-11820.
16. E. G. Buchanan, W. H. James, S. H. Choi, L. Guo, S. H. Gellman, C. W. Muller and T. S. Zwier, *J. Chem. Phys.*, 2012, **137**, 094301.
17. J. C. Dean, E. G. Buchanan and T. S. Zwier, *J. Am. Chem. Soc.*, 2012, **134**, 17186-17201.
18. M. Z. Kamrath, E. Garand, P. A. Jordan, C. M. Leavitt, A. B. Wolk, M. J. Van Stipdonk, S. J. Miller and M. A. Johnson, *J. Am. Chem. Soc.*, 2011, **133**, 6440-6448.
19. B. M. Marsh, E. M. Duffy, M. T. Soukup, J. Zhou and E. Garand, *J. Phys. Chem. A*, 2014, **118**, 3906-3912.
20. N. S. Nagornova, T. R. Rizzo and O. V. Boyarkin, *Angew. Chem.*, 2013, **52**, 6002-6005.
21. J. Oomens and J. D. Steill, *J. Am. Soc. Mass. Spectrom.*, 2010, **21**, 698-706.
22. W. Ronghu and T. B. McMahon, *J. Phys. Chem. B*, 2009, **113**, 8767-8775.
23. J. A. Stearns, C. Seaiby, O. V. Boyarkin and T. R. Rizzo, *PCCP*, 2009, **11**, 125-132.
24. R. C. Dunbar, N. C. Polfer, G. Berden and J. Oomens, *Int. J. Mass spectrom.*, 2012, **330**, 71-77.
25. T. E. Hofstetter, C. Howder, G. Berden, J. Oomens and P. B. Armentrout, *J. Phys. Chem. B*, 2011, **115**, 12648-12661.
26. J. T. O'Brien, J. S. Prell, J. D. Steill, J. Oomens and E. R. Williams, *J. Phys. Chem. A*, 2008, **112**, 10823-10830.
27. J. S. Prell, T. G. Flick, J. Oomens, G. Berden and E. R. Williams, *J. Phys. Chem. A*, 2010, **114**, 854-860.
28. A. B. Wolk, C. M. Leavitt, E. Garand and M. A. Johnson, *Acc. Chem. Res.*, 2014, **47**, 202-210.
29. A. Barth and C. Zscherp, *Q. Rev. Biophys.*, 2002, **35**, 369-430.
30. B. M. Marsh, J. Zhou and E. Garand, *J. Phys. Chem. A*, 2014, **118**, 2063-2071.
31. E. Garribba and G. Micera, *J. Chem. Educ.*, 2007, **84**, 832-835.
32. M. J. Frisch, G. W. Trucks, H. B. Schlegel, G. E. Scuseria, M. A. Robb, J. R. Cheeseman, G. Scalmani, V. Barone, B. Mennucci, G. A. Petersson, H. Nakatsuji, M. Caricato, X. Li, H. P. Hratchian, A. F. Izmaylov, J. Bloino, G. Zheng, J. L. Sonnenberg, M. Hada, M. Ehara, K. Toyota, R. Fukuda, J. Hasegawa, M. Ishida, T. Nakajima, Y. Honda, O. Kitao, H. Nakai, T. Vreven, J. A.

Montgomery, J. E. Peralta, F. Ogliaro, M. Bearpark, J. J. Heyd, E. Brothers, K. N. Kudin, V. N. Staroverov, R. Kobayashi, J. Normand, K. Raghavachari, A. Rendell, J. C. Burant, S. S. Iyengar, J. Tomasi, M. Cossi, N. Rega, J. M. Millam, M. Klene, J. E. Knox, J. B. Cross, V. Bakken, C. Adamo, J. Jaramillo, R. Gomperts, R. E. Stratmann, O. Yazyev, A. J. Austin, R. Cammi, C. Pomelli, J. W. Ochterski, R. L. Martin, K. Morokuma, V. G. Zakrzewski, G. A. Voth, P. Salvador, J. J. Dannenberg, S. Dapprich, A. D. Daniels, Farkas, J. B. Foresman, J. V. Ortiz, J. Cioslowski and D. J. Fox, Wallingford CT, 2009.

33. S. Ataka, H. Takeuchi and M. Tasumi, *J. Mol. Struct.*, 1984, **113**, 147-160.
34. M. K. Kim and A. E. Martell, *Biochemistry*, 1964, **3**, 1169-1174.
35. J. T. O'Brien and E. R. Williams, *J. Phys. Chem. A*, 2008, **112**, 5893-5901.
36. J. Tomasi, B. Mennucci and R. Cammi, *Chem. Rev.*, 2005, **105**, 2999-3093.
37. Z. Ganim, H. S. Chung, A. W. Smith, L. P. Deflores, K. C. Jones and A. Tokmakoff, *Acc. Chem. Res.*, 2008, **41**, 432-441.